Renewable and Sustainable Energy Reviews 30 (2014) 282–289

Contents lists available at ScienceDirect

Renewable and Sustainable Energy Reviews

journal homepage: www.elsevier.com/locate/rser

An improved approach to extract the single-diode equivalent circuit parameters of a photovoltaic cell/panel

Simon Lineykin [a], Moshe Averbukh [b], Alon Kuperman [b,*]

[a] Department of Mechanical Engineering and Mechatronics, Ariel University, 40700, Israel
[b] Department of Electrical Engineering and Electronics, Ariel University, 40700, Israel

ARTICLE INFO

Article history:
Received 24 October 2012
Received in revised form
30 September 2013
Accepted 19 October 2013
Available online 8 November 2013

Keywords:
Lambert function
Single diode solar cell model
Parameters extraction
I–V characteristics

ABSTRACT

The paper offers a novel approach to parameter estimation of a single-diode solar cell/panel equivalent circuit, based on analysis of either technical characteristics supplied by the manufacturer or user-obtained experimental *I–V* curve. The derived model allows predicting the solar cell/panel output for arbitrary environmental conditions. The method combines a solution of an algebraic equations system with an optimization algorithm. The main advantage of the proposed method is that in order to obtain the required parameters of the model, minimal set of experimental data is required. In order to validate the feasibility of the proposed approach, several solar panels of different types from several manufacturers were analyzed. The results demonstrate 0.1–0.5% estimation precision when the Standard Operation Conditions data from the manufacturers' datasheets are employed.

Contents

1. Introduction

Modeling of photovoltaic devices and simulating their behavior represent significant portion of today's research in the field of solar energy. Modeling using an equivalent circuit (lumped parameters model) is of particular interest, since it allows performing joint simulation of a photoelectric device with power electronics interfaces [1–5]. Such simulations allow optimizing the design of solar arrays and power systems and provide valuable assistance during Maximum Power Point Tracking algorithms development without costly experiments but using computer models only [6–8]. Hence, proper selection of an equivalent circuit topology along with suitable methodology of extracting optimal set of equivalent circuit parameters, characterizing a specific device, is a very important part of modeling process.

Dozens of scientific and engineering publications covering a variety of methods for extracting the parameters of equivalent circuit models were revealed recently. Most researchers propose a topology, including both linear and nonlinear components [9]. The linear part consists of resistive elements and irradiation dependent current source. Typically, two equivalent resistors are included: series and shunt/parallel resistances [10–12]. In some cases, the shunt resistance is neglected since it is much larger than the series

* Corresponding author. Tel.: +972 526943234.
E-mail address: alonku@ariel.ac.il (A. Kuperman).

1364-0321/$ - see front matter © 2013 Elsevier Ltd. All rights reserved.
http://dx.doi.org/10.1016/j.rser.2013.10.015

one [13,14]. One or more ideal diodes typically represent the nonlinear part of the equivalent circuit [10,12,15,16].

Two fundamental approaches are used for extracting the model parameters of a solar cell/panel. The first one involves multiple optimization techniques, the most prominent example of which is the least mean squares approach. There, the desired parameters are obtained by minimizing the difference between measured data and the modeled *I–V* curve. The method requires fluency in sophisticated algorithms [17–20,22–24] and returns accurate values of the desired parameters in case a sufficiently large number of reference points of the measured *I–V* curve is available [21,25–27].

Solving systems of algebraic (usually transcendental) equations is the second fundamental approach to parameter extraction of a solar cell/panel equivalent circuit [28,29]. The amount of experimental data used in these methods must match the number of unknown parameters. The equations are established taking into account the constraint that the modeled *I–V* curve should pass through three basic points of the measured *I–V* curve. Additional information such as the derivatives of *I–V* curve at the basic points may be used as well [30–34]. In [13], parameter extraction of a single-diode model was performed by solving a system of four algebraic equations, three of which represent the *I–V* curve passing through a set of the following basic points: short circuit current, open circuit voltage and maximum power. The fourth equation used the fact that the power curve derivative is zero at the maximum power point.

The main advantage of analytical methods is that in order to obtain the required parameters of the equivalent circuit, minimal set of experimental data is required [35]. In many cases, the required parameters could be extracted directly from the manufacturer's data. The method in [13] returns good correspondence between theoretical and empirical data for single crystalline photovoltaic cells and panels for relatively high irradiation levels. However, neglecting the shunt resistance causes significant divergence between the theoretical and real *I–V* curve for low irradiation levels. Moreover, this assumption is invalid for modeling polycrystalline, amorphous silicon, and organic solar cells under any irradiation level.

In the present study, a novel approach is proposed for extracting the single-diode equivalent circuit parameters, combining both above mentioned fundamental approaches, i.e. minimization of divergences between the modeled *I–V* curve and experimental data by fitting and solution of algebraic equations (partially transcendental) system. The approach is not new and has been recently discussed in [51,52]; nevertheless, unlike in the mentioned references, here the diode ideality is used as the fitting parameter since its value resides in a relatively narrow, well-defined region. In addition, no simplifying assumptions are made during the analysis. The proposed method allows reducing the number of simultaneously solved equations to two. The other two parameters can be then obtained by direct calculation, while the fifth parameter is derived through optimization/fitting.

Equivalent circuit of the single diode model adopted in the current study is shown in Fig. 1. The model includes a parallel combination of a photogenerated current source I_{ph}, a diode D, described by the well-known single-exponential Shockley equation [36], a shunt resistance R_{sh} and a series resistance R_s. An arbitrary load is connected to the ports of the model and is characterized by the current and voltage I_L and V_L, respectively.

Note that an analytical solution of system in Fig. 1 does not exist in general case. Utilizing the Lambert-W function simplifies the numerical solution [14,37–39]. This function is the inverse of the function $f(x) = xe^x$, i.e. $W(x) = f^{-1}(x)$, where $W(x)$ is the Lambert-W function. The solution process is consequently simplified since the Lambert-W function is a built-in function in most of the existing

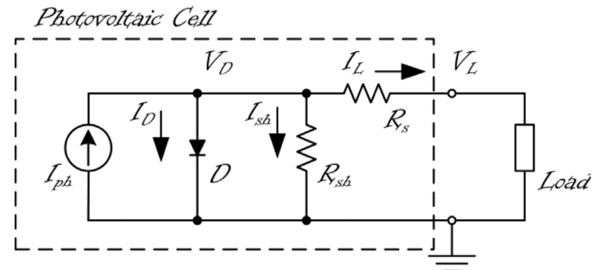


Fig. 1. The "single-diode" equivalent circuit of the photovoltaic cell with a load.

engineering software packages, e.g. *lambert w* in Matlab and *ProductLog* in Mathematica.

A significant contribution of the proposed method is the possibility of obtaining estimated values of band gap energy of the cell and the temperature coefficient of the photo-generating current. The value of the band gap is usually assumed constant; nevertheless, its value varies from one material to another and strongly depends on temperature [40]. Moreover, since the single-diode model only approximates the underlying physical processes, some unmodeled behavior exists in any case and is reflected by variations in band gap value. The information regarding the temperature coefficient of photo-generating current absent from datasheets (the temperature coefficient of the short-circuit current is usually given). Most of the researchers utilize the given coefficient for estimating the photo-generating current for different ambient conditions by assuming that short-circuit current and photo-generating current are equal. Here such assumption is not used. Instead, the temperature coefficient of photo-generating current is analytically calculated. Equations allowing estimating the band gap value and the temperature coefficient of photo-generating current require information regarding temperature coefficients for both open circuit voltage and short circuit current, which are possible to obtain either by test measurements or from manufacturer specifications, as mentioned. Thus, only the electron's charge and the Boltzmann constant are assumed constant in the proposed method.

2. Materials and methods

The proposed methodology consists of four main steps. The first step involves obtaining the *I–V* curve expressions based on the single-diode equivalent circuit, also referred to as "five parameter model". In the second step, substitution of the standard temperature conditions (STC) data into expressions derived during the first step creates a set of four algebraic equations, still insufficient for determining the five parameters of the chosen equivalent circuit. Thus, the fifth parameter is determined by minimization of the difference (i.e. by fitting) between the corresponding sets of modeled and experimental *I–V* curves in the third step. Here, the diode ideality factor is chosen as the fitting parameter [37]. The fourth step involves a solution of two additional equations, in which thermal coefficients of open circuit voltage and short circuit current are utilized to determine the band gap energy and temperature coefficient of the photo-generating current.

It is important to note that all the equations are derived for a single while the manufacturer's data is usually given for a panel. Since a typical solar panel consists of multiple serially connected cells, the panel voltage is scaled down by number of cells to obtain single cell data [41]. Nevertheless, in case a solar panel consists of parallel cell connection, the panel current should be similarly scaled.

3. Theory/calculation

3.1. Deriving the set of equivalent circuit equations

A set of algebraic equations is derived according to Kirchhoff's laws, taking into consideration the characteristic of all circuit elements. The diode current may be described by Shockley's expression [36] as

$$I_D = I_0(e^{(V_D/\eta V_T)} - 1), \tag{1}$$

where V_T [V] is thermal voltage, I_0 [A] is reverse bias saturation current and η is diode ideality factor. The thermal voltage is expressed as

$$V_T = \frac{k_b T}{q} = V_T^* \left(\frac{T}{T^*}\right), \tag{2}$$

where $k_b = 1.380 \times 10^{-23}$ [J K^{-1}] is Boltzmann constant, $q = 1.602 \times 10^{-19}$ [C] is elementary charge and T [K] is cell/panel temperature. The asterisk (*) here and thereafter denotes a value corresponding to STC, i.e. irradiance of 1 kW m^{-2}, AM 1.5 and cell/panel temperature of 25 °C.

The reverse bias saturation current depends on temperature as [42]

$$I_0 = I_0^* \left(\frac{T}{T^*}\right)^3 e^{(E_g/q\ \eta V_T^*)(T - T^*/T)}, \tag{3}$$

where E_g [eV] is the band gap energy. According to [43–45], and [13], the photocurrent is given by

$$I_{ph} = k_{ph} \frac{\Psi}{\Psi^*} I_{ph}^* (1 + \varepsilon(T - T^*)) \tag{4}$$

where ε [K^{-1}] is the temperature coefficient of the photocurrent, Ψ [W m^{-2}] is the irradiance and k_{ph} is the spectral factor ($k_{ph} = 1$ for AM 1.5) [13].

Applying Kirchhoff's laws to Fig. 1, the set of equivalent circuit equations consists of the three following relations,

$$I_{ph} - I_D - I_{sh} - I_L = 0, \tag{5}$$

$$V_D - V_L - I_L R_s = 0, \tag{6}$$

$$I_{sh} = \frac{V_D}{R_{sh}}. \tag{7}$$

Note that resistors R_s and R_{sh} as well as the diode ideality factor η are further assumed to be temperature independent [13]. Combining (1) and (5)–(7) and applying the Lambert-W function, the expression of I–V curve may be presented in the two following forms,

$$V_L = (I_0 + I_{ph}) \cdot R_{sh} - I_L \cdot (R_s + R_{sh}) - \eta \cdot V_T \cdot W\left(\frac{I_0}{\eta \cdot V_T} \cdot R_{sh} \cdot e^{((I_0 - I_L + I_{ph}) \cdot R_{sh}/(\eta \cdot V_T))}\right) \tag{8}$$

and

$$I_L = \frac{(I_0 + I_{ph}) \cdot R_{sh} - V_L}{R_s + R_{sh}} - \frac{\eta \cdot V_T}{R_s} \cdot W\left(\frac{I_0}{\eta \cdot V_T} \cdot \frac{R_s \cdot R_{sh}}{(R_s + R_{sh})} \cdot e^{(R_{sh} \cdot ((I_0 + I_{ph}) \cdot R_s + V_L)/\eta \cdot V_T \cdot (R_s + R_{sh}))}\right) \tag{9}$$

3.2. Substitution of STC data into the I-V curve expressions

Expressions (8) and (9) allow to carry out the calculations for determination of all the five unknown equivalent circuit parameters, namely I_{ph}, I_0, R_s, R_{sh}, and η. The STC data is typically provided by the manufacturer and is utilized as follows. The short circuit current I_{sc}^*, the open circuit voltage V_{oc}^* and the maximum power point voltage–current pair (V_m^*, I_m^*) of the STC I–V curve are referred to as basic points. The manufacturer usually supplies these data in a tabular form; moreover, these points can be easily extracted from the datasheet I–V curve with relatively high precision as well.

Substitution of $I_L = 0$ and $V_L = V_{oc}^*$ into (8) leads to the following open circuit STC relation:

$$V_{oc}^* = (I_0^* + I_{ph}^*) \cdot R_{sh} - \eta \cdot V_T^* \cdot W\left(\frac{I_0^*}{\eta \cdot V_T^*} \cdot R_{sh} \cdot e^{((I_0^* + I_{ph}^*) \cdot R_{sh}/\eta \cdot V_T^*)}\right) \cdot \tag{10}$$

Furthermore, substitution of $V_L = 0$ and $I_L = I_{sc}^*$ into (9) leads to the subsequent short circuit STC expression,

$$I_{sc}^* = \frac{R_s || R_{sh}}{R_s} \cdot (I_0^* + I_{ph}^*) - \frac{\eta V_T^*}{R_s} \cdot W\left(\frac{I_0^*}{\eta V_T^*} \cdot R_s || R_{sh} \cdot e^{R_{sh} || R_s \frac{(I_0^* + I_{ph}^*)}{\eta V_T^*}}\right) \cdot \tag{11}$$

The (V_m^*, I_m^*) voltage–current pair determines the location of maximum power point on the STC I–V curve,

$$V_m^* = V_L(I_m^*). \tag{12}$$

Hence, combining (8) and (12), maximum power point STC relation is given by

$$V_m^* = (I_0^* + I_{ph}^*) \cdot R_{sh} - I_m^* \cdot (R_s + R_{sh}) - \eta \cdot V_T^* \cdot W\left(\frac{I_0^*}{\eta \cdot V_T^*} \cdot R_{sh} \cdot e^{((I_0^* - I_m^* + I_{ph}^*) \cdot R_{sh}/\eta \cdot V_T^*)}\right) \cdot \tag{13}$$

The following condition determines the *extremum* of the power curve at $I_L = I_m^*$:

$$\left.\frac{d(I_L \cdot V_L)}{dI_L}\right|_{I_L = I_m^*} = 0 \cdot \tag{14}$$

Combining of (8) and (14) leads to

$$(I_0^* + I_{ph}^*) \cdot R_{sh} - 2I_m^* \cdot (R_s + R_{sh}) + +W\left(\frac{I_0^* R_{sh}}{\eta \cdot V_T^*} e^{((I_0^* - I_m^* + I_{ph}^*) R_{sh}/\eta \cdot V_T^*)}\right) \cdot \left(\frac{I_m^* R_{sh}}{1 + W((I_0^* \cdot R_{sh}/\eta \cdot V_T^*) \cdot e^{((I_0^* - I_m^* + I_{ph}^*) R_{sh}/\eta \cdot V_T^*)})} - \eta \cdot V_T^*\right) = 0 \cdot \tag{15}$$

To summarize, a system of four transcendental Eqs. (10), (11), (13), and (15) is now derived for STC. Note that the obtained set of equations is still insufficient for complete solution since there are five unknowns.

3.3. Solving the system of equations

A possible way to solve the derived system of equations is treating one of the unknowns as an independent parameter, which may be determined by fulfillment of an additional condition, namely minimization of deviation between the theoretical and measured I–V curves. Each one of the five unknowns may be selected as an independent one, though the ideality factor is probably the most convenient since its value resides in a known bounded range for any type of photovoltaic cells ($1 \le \eta \le 2$ for silicon cells/panels) [37].

Combining (1), (5) and (6) for open and short circuit STC conditions results in

$$I_0^* = \frac{I_{ph}^* \cdot R_{sh} - V_{oc}^*}{R_{sh} \cdot (e^{(V_{oc}^*/\eta \cdot V_T^*)} - 1)} \tag{16}$$

And

$$I_{ph}^* = I_{sc}^* \frac{R_{sh} + R_s}{R_{sh}} + \frac{I_{sc}^*(R_{sh} + R_s) - V_{oc}^*}{R_{sh}} \cdot \frac{e^{(I_{sc}^* R_s/\eta V_T^*)} - 1}{e^{(V_{oc}^*/\eta V_T^*)} - e^{(I_{sc}^* R_s/\eta V_T^*)}}, \tag{17}$$

respectively. Substitution of (16) and (17) into (13) and (15) results in the system of two transcendental equations with three unknowns R_s, R_{sh} and η, where η is an independent parameter, residing within a known range. The system of these two transcendental equations is solvable only by numerical methods. Each value of η creates a specific set of (R_s, R_{sh}), for which I_0^* and I_{ph}^* may be found from (16) and (17). Each full set of five parameters

determines a specific *I–V* curve that passes through the three basic points and possesses a maximum power point at (I_m, V_m) as shown in Fig. 2. Certain deviation exists between the curves except at the three basic points, where the curves must coincide. The correct value of η corresponds to the modeled curve with minimum deviation from the datasheet/measured *I–V* curve at STC.

The minimization may be performed by visual comparison between modeled curves and the measured one as well as by the simplest error minimization algorithm. When a measured *I–V* curve is unavailable in raw data form and a datasheet picture only is available (which is a typical case), one can use digitizer software, e.g. [45], which helps digitizing scanned plots into a raw data with fair precision.

3.4. Additional set of equations for thermal parameters calculation

The first three steps allow a fairly accurate reproduction of the STC *I–V* curve. The final step is estimating *I–V* curves for arbitrary environmental conditions using temperature coefficients. The expression for the open circuit voltage temperature coefficient (TCV_{oc}) can be obtained by combining the derivative of (8) with (2)–(4) and substituting $T=T^*$,

$$\left.\frac{dV_L}{dT}\right|_{T=T^*}=\frac{E_g I_0^* R_{sh}+qR_{sh}(3I_0^*+I_{ph}^*T^*\varepsilon)\eta V_T^*-\eta V_T^* A(E_g-qR_{sh}(I_0^*+I_{ph}^*-I_L)+3q\eta V_T^*+q\eta V_T^* A)}{\eta V_T^*(A+1)qT^*}, \tag{18}$$

where

$$A=W\left(\frac{I_0^* R_{sh}}{\eta V_T^*}e^{(R_{sh}(I_0^*+I_{ph}^*-I_L)/\eta V_T^*)}\right). \tag{19}$$

The TCV_{oc} is obtained from (18) by substituting $I_L=0$ as

$$TCV_{oc}=\frac{E_g I_0^* R_{sh}+qR_{sh}(3I_0^*+I_{ph}^*T^*\varepsilon)\eta V_T^*-\eta V_T^* B(E_g-qR_{sh}(I_0^*+I_{ph}^*)+3q\eta V_T^*+q\eta V_T^* B)}{\eta qT^* V_T^*(B+1)} \tag{20}$$

where

$$B=W\left(\frac{I_0^* R_{sh}}{\eta V_T^*}e^{(R_{sh}(I_0^*+I_{ph}^*)/\eta V_T^*)}\right). \tag{21}$$

Similarly, the expression for the short circuit current temperature coefficient (TCI_{sc}) may be derived from combining the derivative of (9) with (2)–(4) and substituting $T=T^*$,

$$TCI_{sc}=\left.\frac{dI_L}{dT}\right|_{T=T^*}=\frac{R_s||R_{sh}}{\eta V_T^* qR_s T^*(C+1)}\cdot\left(E_g I_0^*+\eta V_T^* q(3I_0^*+I_{ph}^*T^*\varepsilon)+q(I_0^*+I_{ph}^*)-\frac{E_g-3\eta V_T^* q-\eta V_T^* qC}{R_{sh}||R_s}+\frac{\eta V_T^*}{R_s R_{sh}}C\right) \tag{22}$$

where

$$C=W\left((R_s||R_{sh})\frac{I_0^*}{\eta V_T^*}e^{((I_0^*+I_{ph}^*)(R_s||R_{sh})/\eta V_T^*)}\right) \tag{23}$$

The values of E_g and ε can be then obtained by solving (20) and (22).

4. Results and discussion

The proposed method was first applied to Isofoton IS – 160 mono-crystalline solar panel [46]. The seven parameters of the model (R_s, R_{sh}, I_0^*, I_{ph}^*, η, E_g and ε) were obtained in accordance with the four steps of the presented approach. Theoretical *I–V* curves derived using the proposed method for different environmental conditions were compared to experimental *I–V* data provided by manufacturer. All the equivalent circuit parameters were obtained from the manufacturer's data only. The results were obtained for the same environmental conditions as manufacturers' and transferred into transparent *I–V* curve plots. These plots were superimposed with the manufacturers' datasheets by corresponding scaling along each axis.

The specifications of the IS – 160 panel and the manufacturer's *I–V* curve are shown in Table 1 and Fig. 3, respectively. Note that the data, provided by Isofoton in tabular form and the datasheet *I–V* curve slightly differ (common to different solar panels manufacturers). The deviation remains within the tolerance (±5%) declared by the manufacturer.

Since the proposed method is very sensitive to input data, graphical data was used here rather than tabular one. The estimation procedure was carried out using Mathematica software [47]. The estimation results for STC are summarized in Table 2.

The estimated parameters, given in Table 2, were used for creating modeled *I–V* and *P–V* curves for STC (Fig. 4) and different temperatures (Fig. 5). Good agreement may be observed, characterized by deviations of 0.1–0.5%.

Furthermore, the proposed method was applied to three additional solar panels, specified in Tables 3–5. The estimation results are summarized in Tables 6–8. The corresponding *I–V* and

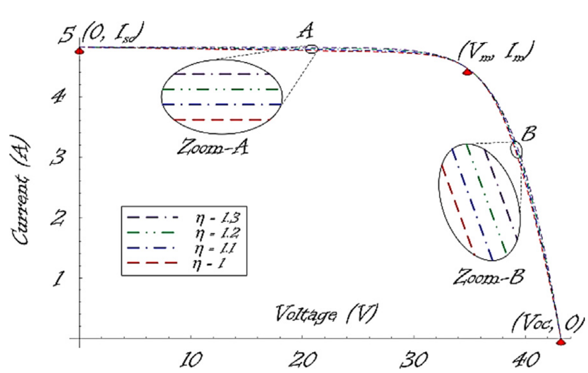


Fig. 2. The family of *I–V* curves with different ideality factors passing through the basic points

Table 1
Specification of the IS – 160 solar panel [46].

Electrical characteristics, STC	From datasheet table	From datasheet *I–V* curve
Number of series-connected cells n_s	72	72
Maximum power P_m, [W]	160 (±3%)	155.67
Maximum power voltage V_m, [V]	35	35.2
Maximum power current I_m, [A]	4.57	4.42
Shot circuit current I_{sc}, [A]	4.9	4.81
Open circuit voltage V_{oc}, [V]	43.8	43.2
Temperature coefficient of V_{oc}, %/K	−0.378	−0.353
Temperature coefficient of I_{sc}, %/K	0.0254	0.0254

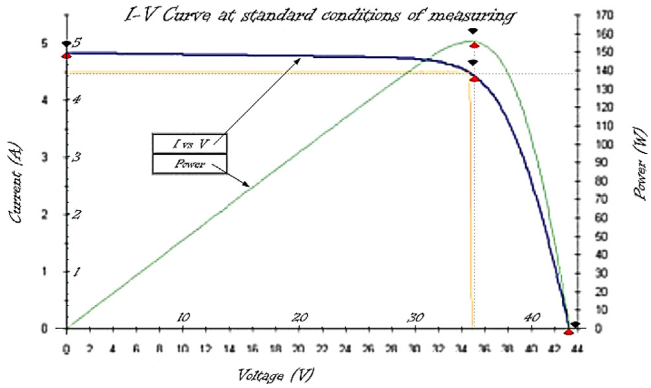


Fig. 3. The STC *I*–*V* curve of IS – 160 panel, digitized from the datasheet.

Table 2
The estimated STC parameters for a single cell of the IS-160 panel.

Parameter	Estimated value
Ideality factor, η	1.0
Series resistance R_s, [mΩ]	8.0
Shunt resistance R_{sh}, [Ω]	3.25
Photocurrent I_{ph}, [A]	4.824
Reverse bias saturation current I_0, [μA]	0.33
Band gap energy E_g, [eV]	1.16
Temperature coefficient of I_{ph}, [μA/K]	254

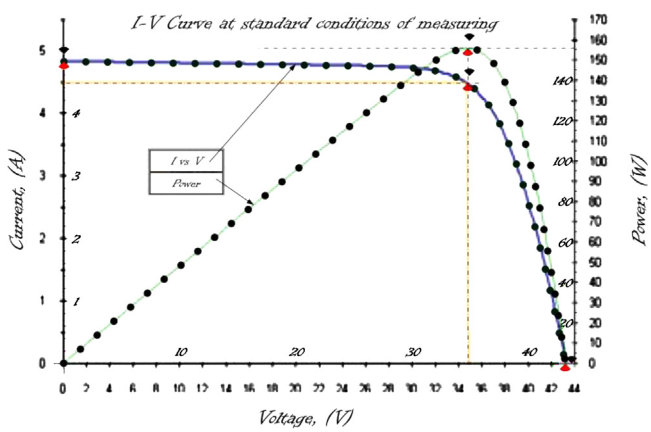


Fig. 4. The *I*–*V* and power curves of IS-160 at STC. Simulation results (dotted) are added to the manufacturer's data (solid).

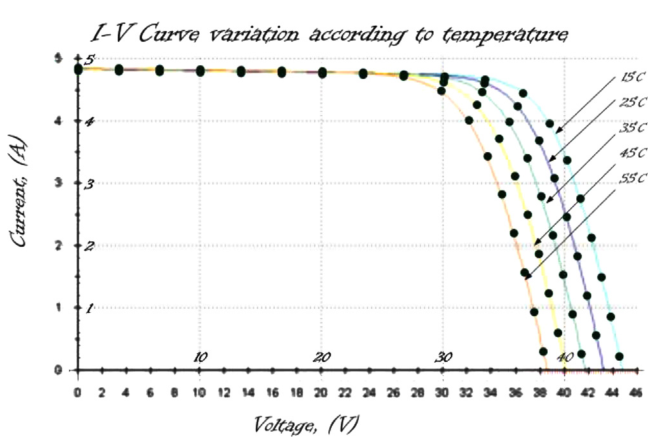


Fig. 5. The *I*–*V* and power curves of IS-160 for different temperatures. Simulation results (dotted) are added to the manufacturer's data (solid).

Table 3
Specification of the Suntech CNPV-280P solar panel [48].

Electrical characteristics, STC	From datasheet *I*–*V* curve
Number of series-connected cells n_s	72
maximum power P_m, [W]	280
Maximum power voltage V_m, [V]	36.9
Maximum power current I_m, [A]	7.6
Shot circuit current I_{sc}, [A]	8.2
Open circuit voltage V_{oc}, [V]	44.6
Temperature coefficient of V_{oc}, %/K	−0.3
Temperature coefficient of I_{sc}, %/K	0.05

Table 4
Specification of the Schuco SF-160-24-M175 solar panel [49].

Electrical characteristics, STC	From datasheet *I*–*V* curve
Number of series-connected cells n_s	72
Maximum power P_m, [W]	175
Maximum power voltage V_m, [V]	36
Maximum power current I_m, [A]	4.86
Shot circuit current I_{sc}, [A]	5.2
Open circuit voltage V_{oc}, [V]	44.8
Temperature coefficient of V_{oc}, %/K	−0.48
Temperature coefficient of I_{sc}, %/K	0.04

Table 5
Specification of the Kyocera KC200GT solar panel [50].

Electrical characteristics, STC	From datasheet *I*–*V* curve
Number of series-connected cells n_s	54
Maximum power P_m, [W]	200
Maximum power voltage V_m, [V]	26.3
Maximum power current I_m, [A]	7.61
Shot circuit current I_{sc}, [A]	8.21
Open circuit voltage V_{oc}, [V]	32.9
Temperature coefficient of V_{oc}, %/K	−0.374
Temperature coefficient of I_{sc}, %/K	0.039

Table 6
The estimated STC parameters for a single cell of the CNPV-280P panel.

Parameter	Estimated value
Ideality factor, η	1.0
Series resistance R_s, [mΩ]	4.2
Shunt resistance R_{sh}, [Ω]	4.3
Photocurrent I_{ph}, [A]	8.19
Reverse bias saturation current I_0, [nA]	0.27
Band gap energy E_g, [eV]	1.19
Temperature coefficient of I_{ph}, [μA/K]	420

power curves of these panels along with the manufacturers' supplied data are shown in Figs. 6–8. It can be concluded that the estimated curves nearly coincide with the manufacturer provided curves, indicating the feasibility and high precision of the proposed method.

5. Conclusions

An improved method for determining the parameters of single-diode photovoltaic cell equivalent circuit was developed in the

Table 7
The estimated STC parameters for a single cell of the SF-160-24-M175 panel.

Parameter	Estimated value
Ideality factor, η	1.2
Series resistance R_s, [mΩ]	7.1
Shunt resistance R_{sh}, [Ω]	10.2
Photocurrent I_{ph}, [A]	5.18
Reverse bias saturation current I_0, [nA]	10.2
Band gap energy E_g, [eV]	1.16
Temperature coefficient of I_{ph}, [μA/K]	300

Table 8
The estimated STC parameters for a single cell of the KC200GT panel.

Parameter	Estimated value
Ideality factor, η	1.05
Series resistance R_s, [mΩ]	4.85
Shunt resistance R_{sh}, [Ω]	3.6
Photocurrent I_{ph}, [A]	8.2
Reverse bias saturation current I_0, [nA]	1.05
Band gap energy E_g, [eV]	1.22
Temperature coefficient of I_{ph}, [μA/K]	388

presented work. The set of experimental data required for the extraction of model parameters included manufacturer provided STC data only.

In order to calculate the five unknown parameters for STC conditions, the method combined a solution of algebraic equations system to obtain four unknown parameters; whereas the fifth parameter was obtained by minimization of the divergence between the modeled and experimental *I–V* curves. Two additional "thermal" parameters were derived from the solution of another system of algebraic equations based on the solar cell/panel temperature coefficients. A number of *I–V* curve points besides the three basic points (short and open circuits, maximum power) were required to obtain an accurate estimation of the ideality factor. One can obtain these points directly from the STC *I–V* curve available in the cell/panel datasheet. For this purpose, dedicated digitizing software was applied.

Since the accuracy of the model parameters strongly depends on the accuracy of the input data, the accuracy of the data offered by the manufacturer (typically 3%) is not always enough. The precision has to be in the 1–1.5% range for obtaining correct model parameters. High accuracy of the temperature coefficients is also necessary. Correction of manufacturer provided is often necessary and may be performed by deriving these parameters from the manufacturer provided graphical data.

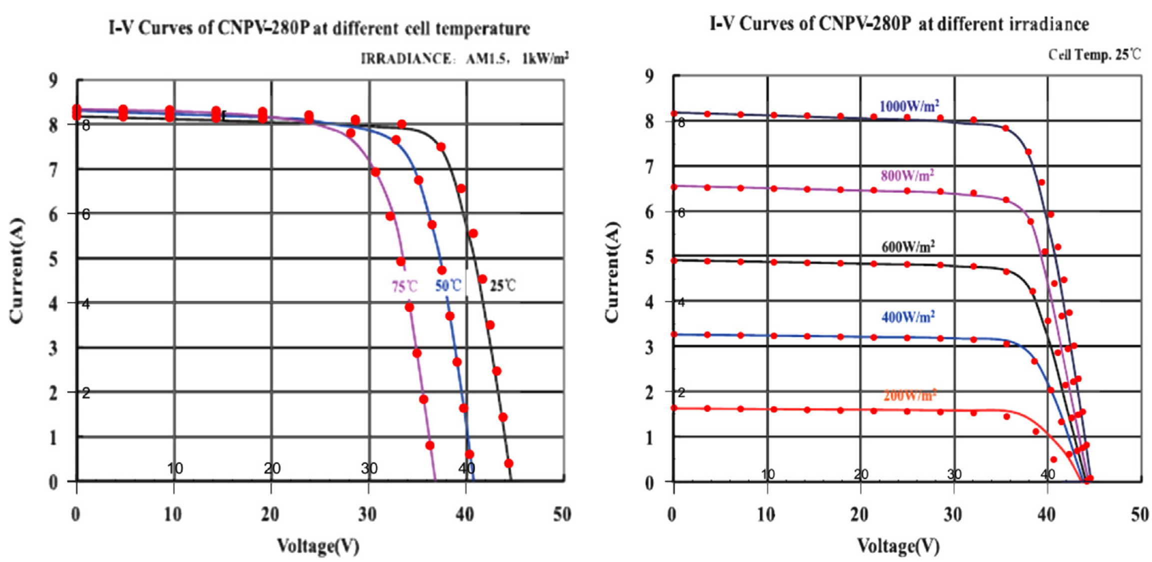


Fig. 6. The *I–V* curves of CNPV-280P for different irradiance levels and temperatures. Simulation results (dotted) are added to the manufacturer's data (solid).

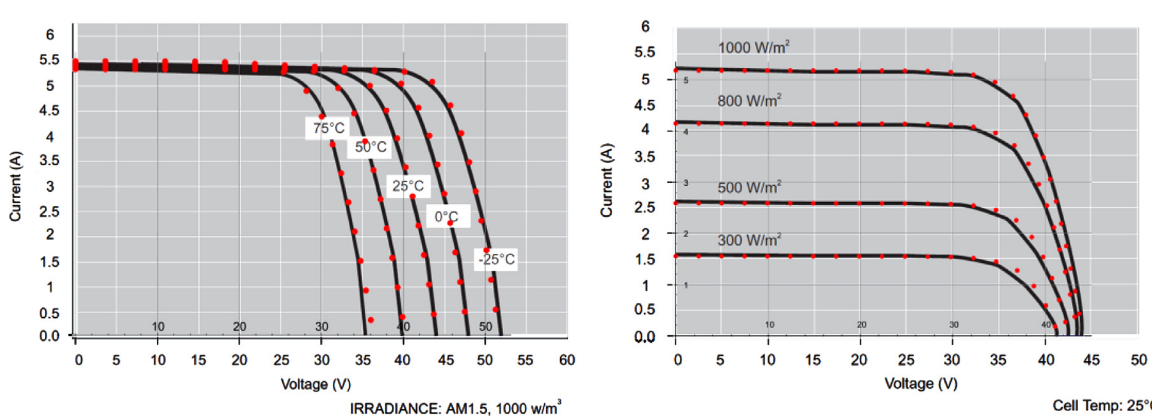


Fig. 7. The *I–V* curves of SF 160-24-M for different irradiance levels and temperatures. Simulation results (dotted) are added to the manufacturer's data (solid).

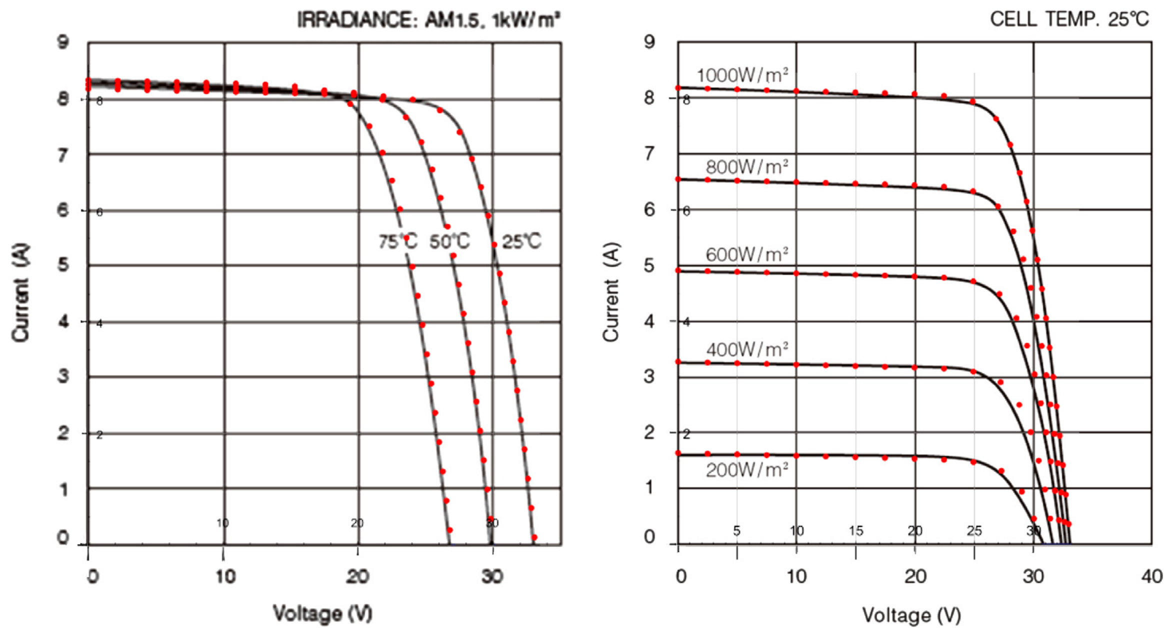


Fig. 8. The *I–V* curves of KC200GT for different irradiance levels and temperatures. Simulation results (dotted) are added to the manufacturer's data (solid).

The proposed method was verified by comparison between modeled and datasheet *I–V* curves of several off the shelf panels of leading manufacturers. The results demonstrated average deviation of 0.1–0.5%, indicating the proposed method feasibility and high accuracy.

References

[1] Li Y, Huang W, Huang H, Hewitt C, Chen Y, Fang G, et al. Evaluation of methods to extract parameters from current-voltage characteristics of solar cells. Sol Energy 2013;90:51–7.
[2] Maffezzoni P, Codecasa L, D'Amore D. Modeling and simulation of a hybrid photovoltaic module equipped with a heat-recovery system. IEEE Trans Ind Electron 2009;56:4311–8.
[3] Dondi D, Bertacchini A, Brunelli D, Larcher L. Modeling and optimization of a solar energy harvester system for self-powered wireless sensor networks. IEEE Trans Ind Electron 2008;55:2759–66.
[4] N.D. Benavides, Chapman PL. Modeling the effect of voltage ripple on the power output of photovoltaic modules. IEEE Trans Ind Electron 2008;55:2638–43.
[5] M.F. AlHajri, K.M. El-Naggar, M.R. AlRashidi, Al-Othman AK. Optimal extraction of solar cell parameters using pattern search. Renew Energy 2012;44:238–45.
[6] Averbukh M, Ben-Galim Y, Uhananov A. Development of quick dynamic response maximum power point tracker algorithm for off-grid system with adaptive switching (on-off) control of dc/dc converter. J Sol Energy Eng 2013;135:021003.
[7] Kadri R, Gaubert JP, Champenois G. An improved maximum power point tracking for photovoltaic grid-connected inverter based on voltage-oriented control. IEEE Trans Ind Electron 2011;58:66–75.
[8] Scarpa V, Buso S, Spiazzi G. Low-complexity MPPT technique exploiting the PV module MPP locus characterization. IEEE Trans Ind Electron 2009;56:1531–8.
[9] Ortiz-Conde A, Garcia-Sanchez FJ. Approximate analytical expression for the equation of the ideal diode with series and shunt resistances. Electron Lett 1992;28:1964–5.
[10] Chan DS, Phang JC. Analytical methods for the extraction of solar-cell single- and double-diode model parameters from *I–V* characteristics. IEEE Trans Electron Dev 1987;34:286–93.
[11] Yadir S, Benhmida M, Sidki M, Assaid E, Khaidar M New method for extracting the model physical parameters of solar cells using explicit analytic solutions of current-voltage equation. In: Proceedings of international conference on microelectronics 2009, p. 390–3.
[12] Ortiz-Conde A, García-Sánchez FJ. An explicit multiexponential model as an alternative to traditional solar cell models with series and shunt resistances. IEEE J Photovolta 2012;2:261–8.
[13] Averbukh M, Lineykin S, Kuperman A. Obtaining small photovoltaic array operational curves for arbitrary cell temperatures and solar irradiation densities from standard conditions data. Prog Photovolt: Res Appl 2013;21:1016–24.
[14] Banwell TC, Jayakumar A. Exact analytical solution for the current flow through diode with series resistance. Electron Lett 2000;36:291–2.
[15] Vokas GA, Machias AV, Souflis JL. Computer modeling and parameters estimation. In: Proceedings of the 6th IEEE mediterranean electrotechnical conference 1991, p. 206–9.
[16] Ortiz-Conde A, García-Sánchez FJ, Terán Barrios A, Muci J, de Souza M, Pavanello MA. Approximate analytical expression for the terminal voltage in multi-exponential diode models. Solid-State Electron 2013;89:7–11.
[17] Moldovan N, Picos R, Garcia-Moreno E. Parameter extraction of a solar cell compact model using genetic algorithms. In: Proceedings of Spanish conference on electronic devices 2009, p. 379–82.
[18] Ishaque K, Salam Z, Taheri H, Shamsudin A. Parameter extraction of photovoltaic cell using differential evolution method. In: Proceedings of IEEE applied power electronics colloquium 2011, p. 10–5.
19] Kennerud KL. Analysis of performance degradation in CdS solar cells. IEEE Trans Aerosp Electron Syst 1969;5:912–7.
[20] Ishaque K, Salam Z, Taheri H, Shamsudin A. A critical evaluation of EA computational methods for photovoltaic cell parameter extraction based on two—diode model. Sol Energy 2011;85:1768–79.
[21] Ishibashi K, Kimura Y, Niwano M. An extensively valid and stable method for derivation of all parameters of a solar cell from a single current–voltage characteristic. J Appl Phys 2008;103:094507.
[22] Bendib T, Djeffal F, Arar D, Meguellati M. Fuzzy-Logic-based approach for organic solar cell parameters extraction. In: Proceedings of world congress on engineering 2013, p. 1182–5.
[23] Siddiqui MU, Abido M. Parameter estimation for five and seven parameter photovoltaic electrical models using evolutionary algorithms. Appl Soft Comput 2013;13(12):4608–21.
[24] Jiang LL, Maskell DL, Patra JC. Parameter estimation of solar cells and modules using an improved adaptive differential evolution algorithm. Appl Energy 2013;112:185–93.
[25] AlRashidi MR, AlHajri MF, K.M. El-Naggar, Al-Othman AK. A new estimation approach for determining the *I–V* characteristics of solar cells. Sol Energy 2011;85:1543–50.
[26] Kassis A, Saad M. Analysis of multi-crystalline silicon solar cells at low illumination levels using a modified two-diode model. Sol Energy Mater Sol Cells 2010;94:2108–12.
[27] Marion B, Rummel S, Anderberg A. Current–voltage curve translation by bilinear interpolation. Prog Photovolt: Res Appl 2004;12:593–607.
[28] Lo Brano V, Orioli A, Ciulla G, Di Gangi A. An improved five-parameter model for photovoltaic modules. Sol Energy Mater Sol Cells 2010;94:1358–70.
[29] Schumacher J, Eicker U, Piedrushcka D, Catani A. Exact analytical calculation of the one diode model parameters from PV module data sheet information. In: Proceedings of 22nd European photovoltaic solar energy conference 2007, p. 3212–7.
[30] Phang JC, Chan DS, Phillips JR. Accurate analytical method for the extraction of solar cell model parameters. Electron Lett 1984;20:406–8.
[31] Saraiva S, Melício R, Matias J, Cabrita C, Catalão JP. Simulation and experimental results for a photovoltaic system formed by polycrystalline solar modules. In: Proceedings of the 16th IEEE mediterranean electrotechnical conference 2012, p. 806–9.
[32] Seddaoui, N, Rahmani L, Chauder A, Kessal A. Parameters extraction of photovoltaic module at reference and real conditions. In: Proceedings of the 46th international universities power engineering conference 2011, p. 1–6.

[33] Wang B, Li A, Xiang T, Zhang J, Chen H. An approach of parameters calculation based on monocrystalline silicon photovoltaic cells. In: Proceedings of IEEE Asia-pacific power and energy engineering conference 2011, p. 1–4.
[34] Dongue SB, Njomo D, Ebengai L. A new strategy for accurately predicting electrical characteristics of PV modules using a nonlinear five-point model. J Energy 2013 Article ID: 321694, http://dx.doi.org/10.1155/2013/321694.
[35] Durán E Piliougine M, Sidrach-de-Cardona M, Galán J, Andújar JM. Different methods to obtain the *I–V* curve of PV modules: a review. In: Proceedings of the 33rd IEEE photovoltaic specialists conference 2008, p. 1–6.
[36] Sah CT, Noyce RN, Shockley W. Carrier generation and recombination in *P–N* junctions and *P–N* junction characteristics. Proc IRE 1957;45:1228–43.
[37] Jain A, Kapoor A. A new method to determine the diode ideality factor of real solar cell using Lambert W-function. Sol Energy Mater Sol Cells 2005;85: 391–6.
[38] Zhang ZZ, Cheng XF, Liu JL. An improvement method for extracting five parameters of a solar cell based on Lambert W function with the current-voltage data. Appl Mech Mater 2013;291:38–42.
[39] Ghani F, Duke M. Numerical determination of parasitic resistances of a solar cell using the Lambert W function,. Sol Energy 2011;85:2386–94.
[40] Sze SM. The physics of semiconductor devices. New York: Wiley; 1969.
[41] Tian H, Mancilla-David F, Ellis K, Muljadi E, Jenkins P. A cell-to-module-to-array detailed model for photovoltaic panels. Sol Energy 2012;86:2695–706.
[42] Attivissimo F, Di Nisio A, Savino M, Spadavecchia M. Uncertainty analysis in photovoltaic cell parameter estimation. IEEE Trans Instrum Measurement 2012;61:1334–42.
[43] Saloux E, Teyssedou A, Sorin M. Explicit model of photovoltaic panels to determine voltages and currents at the maximum power point. Sol Energy 2011;85:713–22.
[44] da Costa WT, Fardin JF, Neto VB. Identification of photovoltaic model parameters by differential evolution. In: Proceedings of IEEE international conference on industrial technology 2010, p. 931–6.
[45] 〈http://digitizer.sourceforge.net〉.
[46] 〈http://www.isofoton.com〉.
[47] 〈http://www.wolfram.com/mathematica〉.
[48] 〈http://eu.suntech-power.com〉.
[49] 〈http://www.schuco-usa-brochures.com〉.
[50] 〈http://www.kyocerasolar.com〉.
[51] Villalva MG, Gazoli JR, Filho ER. Comprehensive approach to modeling and simulation of photovoltaic arrays. IEEE Trans Power Electron 2009;24:1198–208.
[52] Mahmoud Y, Xiao W, Zeineldin H. A parameterization approach for enhancing PV model accuracy. IEEE Trans Ind Electron 2013;60:5708–16.